ARTICLE

Empirical DFT model to predict triplet quantum yield through singlet-oxygen yields

Bret A. Steinkamp, Luke V. Lutkus, Rob Lewis and Theresa M. McCormick*[a]

[a] Dr. Theresa M. McCormick, PhD
Department of Chemistry
Portland State University
Portland, Oregon 97207, USA
E-mail: t.m.mccormick@pdx.edu

Supporting information for this article is given via a link at the end of the document.

Abstract: Triplet-photosensitizers can be used for a variety of applications, including photocatalysis, OLEDs, and photodynamic therapy. Excited triplet-states can be quenched by triplet-oxygen to make singlet-oxygen. Often the singlet-oxygen quantum yield (Φ_Δ) is used as a lower approximation for the triplet-yield. Unpredictable effects of even minor structural changes can drastically alter the Φ_Δ and complicate the design of new triplet-photosensitizers. The most common strategy to increase Φ_Δ is to incorporate heavy atoms, promoting the "heavy-atom-effect". However, the position and the identity of the heavy atom greatly influences the Φ_Δ. We have created a predictive model that correlates calculated natural atomic orbital composition of the heavy-atom(s) contributing to the frontier molecule orbitals of a photosensitizer with the experimental Φ_Δ. The model, derived from several fluorescein derivatives, provides a calculated Φ_Δ in agreement with the experimental values for a variety of well-known photosensitizers, including rhodamine dyes, fluorescein derivatives, and octahedral metal complexes.

Introduction

Triplet chromophores are important for many aspects of photochemistry including photocatalysis, artificial photosynthesis, organic light-emitting diodes (OLEDs), and biomedical molecular imaging.[1] Recently, focus has been on creating environmentally friendly, inexpensive, and energy efficient organic photosensitizers.[1c,2] Small structural changes can lead to significant impacts on the photophysical properties complicating the design of new chromophores with targeted of photophysical properties.[3] Specifically, the triplet quantum yield (number of excited triplet states formed per absorbed photon) can shift unexpectedly with structural modifications.

The triplet quantum yield is determined by a combination of the rate of intersystem crossing (ISC) and other competing quenching pathways. A main focus in creating more efficient phosphorescent molecules is through faster rates of ISC.[2a,4] The most common method to increase ISC is to increase the spin-orbit coupling (SOC). It is well known that heavy atoms increase SOC, thus increasing ISC, through the heavy atom effect.[5] However, heavy atoms are often less abundant heavy metals, such as Ru and Ir, which are not desirable for 'green' chromophore design. Nevertheless, these organometallic chromophores are often used due to the tuneability of their photophysical properties through ligand modification.[6] A separate approach is to employ heavy halogens as substituents or heavy chalcogens in the ring structure of organic chromophores.[1a,7] It has been shown that the placement of the heavy atoms in a chromophore can have significant impacts on the quantum yield, which is somewhat counterintuitive to the heavy atom effect which assumes that the identity of the heavy atom rather than the position should improve SOC to promote ISC.[8]

One theory is that the contribution of the heavy atoms to the LUMO effects the triplet quantum yield. A previous study into the effect of heavy atom contribution to the frontier molecular orbitals on the triplet yields of chromophores has shown that the position, not just the identity, of the heavy atoms greatly impacts the singlet oxygen quantum yield (Φ_Δ).[9] Schanze *et al.* correlated the increased orbital contribution of the heavy atom to the LUMO and a decrease in the HOMO-LUMO energy gap. However, this previous work only investigated S and Se substitution in a 4,7-bis(2-thienyl)-2,1,3-benzothiadizaole (TBT) structure, and did not consider other types of triplet chromophores.[9]

With expanding demand for more efficient and tuned triplet chromophores, comes a desire to theoretically model and predict triplet yield.[2b] Some have used density functional theory (DFT) calculations based on SOC or ISC.[7b,10] However, these systems require significant computational power and a high degree of specialized knowledge. Due to this complexity, many chemists still turn to experimental photophysical studies for chromophore development, often involving the synthesis of many dyes with varying functional groups.[4,11a] A suite of experiments are required for each compound to determine their photophysical properties; often followed by new synthesis to combine positive effects or to further probe why differences were observed. These studies can be extremely time and resource intensive. Research into how small substituent changes affect the triplet yields has generally been done on a single structural skeleton.[10a,11] Because the population of the excited triplet-state depends on both SOC and the energy difference between the S_1 and T_n states (ΔE_{ST}), the effects of substituent changes on one compound do not always correlate to similar effects or magnitudes on a class of different chromophores, especially when comparing organic dyes to organometallic ones.

Fluorescein derivatives containing bromine and iodine substituents (such as Rose Bengal and Eosin Y) have increased Φ_Δ and decreased fluorescence quantum yields when compared with non-halogenated or chlorinated fluorescein derivatives.[4] This is due to the heavy atom effect of Br and I increasing rates of ISC causing increased Φ_Δ. Unexpectedly, the Φ_Δ does not directly correlate with the number or identity of the halogens. Thus, it would be desirable to quantify the effects of the identity and

position of heavy atoms on Φ_Δ. This study aims to use simple DFT calculations to create a generic predictive model to easily determine Φ_Δ, as a lower bound approximation for the triplet yield that can be used to guide experimental chromophore design.

In this work, we have investigated how the placement and identity of a heavy atom effects the Φ_Δ for a variety of chromophores. Using simple DFT calculations for a series of fluorescein derivatives we have created a model that can predict approximate triplet yields in heavy atom containing chromophores. We have used the Φ_Δ as a lower approximation for the triplet quantum yield (Φ_t) and compared this experimental parameter to computationally determined heavy-atom contribution to the frontier molecular orbitals involved in the first excitation. This model was able to accurately predict the Φ_Δ of novel halogenated fluorescein derivatives while changing both the halogen and its position. Furthermore, the empirically created model predicted agreeable values for the Φ_Δ of a variety of heavy atom containing chromophores, including Ru and Ir based chromophores.

Results and Discussion

Seven halogenated fluorescein dyes, Figure 1, were chosen to create the model with varied H, Cl, Br, and I atoms at positions R_1, R_2, and R_3 as shown in Table 1. These dyes were chosen based on availability of reliable photophysical data in the literature. The structure of each dye was optimized with DFT using B3LYP level of theory and a 6-311+G(d) basis set (LANL2DZ for Ru, Te, I, and Ir). A NBO calculation was used to determine the atomic orbital contribution to each frontier molecular orbital.

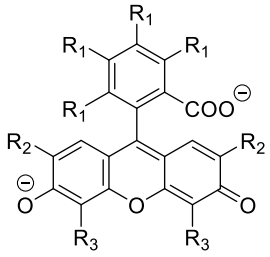

Figure 1. Halogenation pattern of fluorescein derivatives used for developing the model where R_1, R_2, and R_3 are H, Cl, Br, or I as shown in Table 1.

The contribution of the atomic orbitals of each heavy atom to the frontier molecular orbitals were obtained from Multiwfn as a percentage for each atom greater than S.[12] These percentages were converted to a ratio and then adjusted by their atomic number (Z). Next, the contribution was summed for both the occupied and unoccupied orbitals contributing to the first excited state (equation 1). We labeled the unitless value obtained from this calculation as the adjusted heavy atom contribution (AHAC):

$$\mathrm{AHAC} = \sum \left(\frac{\%\ Contribution}{100} \times Z_{Heavy\ Atom} \right). \qquad (1)$$

The typical relationship between SOC and Z^4, does not provide a good fit in this model which uses just Z.[13] It should be noted that this is a model for the singlet oxygen quantum yield, Φ_Δ, and the rate of ISC is not always directly proportional to Φ_Δ. However, the Φ_Δ is often used to approximate the population of the triplet-state due to the relatively simple experimental set-up.[14]

Table 1. Fluorescein derivatives and their experimental Φ_Δ measured in H_2O used to create the predictive model. Substituents are indicated as depicted in Figure 1.

Fluorescein Derivative	R_1	R_2	R_3	Φ_Δ[15]
3',4',5',6'-tetrabromo fluorescein (**TBr**)	Br	H	H	0.20
4,5-dibromo fluorescein	H	H	Br	0.42
4,5-diiodo fluorescein	H	H	I	0.48
Eosin Y	H	Br	Br	0.57
Phloxine B	Cl	Br	Br	0.65
Erythrosine	H	I	I	0.68
Rose Bengal	Cl	I	I	0.76

Due to fast and efficient quenching of the triplet-excited state by triplet oxygen, the use of singlet oxygen yield is an accepted method to approximate the triplet yield.[10a] Finally, the AHAC was plotted against the experimentally reported Φ_Δ. A reciprocal trendline between these points was determined with an asymptote placed at Φ_Δ=1 to account for the limit of Φ_Δ not being greater than 100%.

After the model was created, we tested its predictive powers using a variety of common and less common known chromophores included in Figure 2. The testing was achieved by solving for the AHAC, equation 1, through the same computational process used on the initial halogenated fluorescein derivatives. Next the predicted Φ_Δ was calculated through the trendline, equation 2. Compounds with "heavy atoms" as small as S were tested. The calculated Φ_Δ were then compared to experimental values. Novel halogenated fluorescein derivates, Octabromo-fluorescein (**OBr**) and 3',4',5',6'-tetrachloro-4,5-diiodo fluorescein (**FI**), were synthesized as a first step towards testing the predictive power of the model. A tellurorhodamine dye (**Te1**) was chosen due its frequent use in our lab and methylene blue (**MB**) as a common triplet photosensitizer. Tris(bipyridine)ruthenium(II) (**Ru(bpy)$_3$**) and Tris(2-phenylpyridine)iridium(III) (**Ir(ppy)$_3$**) were chosen to test how the model functions with transition-metal complexes.

Creating the Model

It is often understood that heavy atoms are able to promote ISC to create excited triplet states. However, it is unclear on how the identity and position of these atoms influences the observed Φ_Δ. A simple inspection of the fluorescein derivatives we used would lead one to believe that the tetra-brominated derivative would have a higher Φ_Δ than the di-brominated version. Surprisingly, this is not observed experimentally, with the 3',4',5',6' tetra-brominated fluorescein having a Φ_Δ of 0.20 and the 4,5 di-brominated 0.42.[15] We wanted to know if the contribution of the heavy atom to the frontier molecular orbitals could be used to predict the Φ_Δ. We began by determining the heavy atom contribution to the frontier orbitals of the seven chosen fluorescein derivatives in both singlet and triplet states.

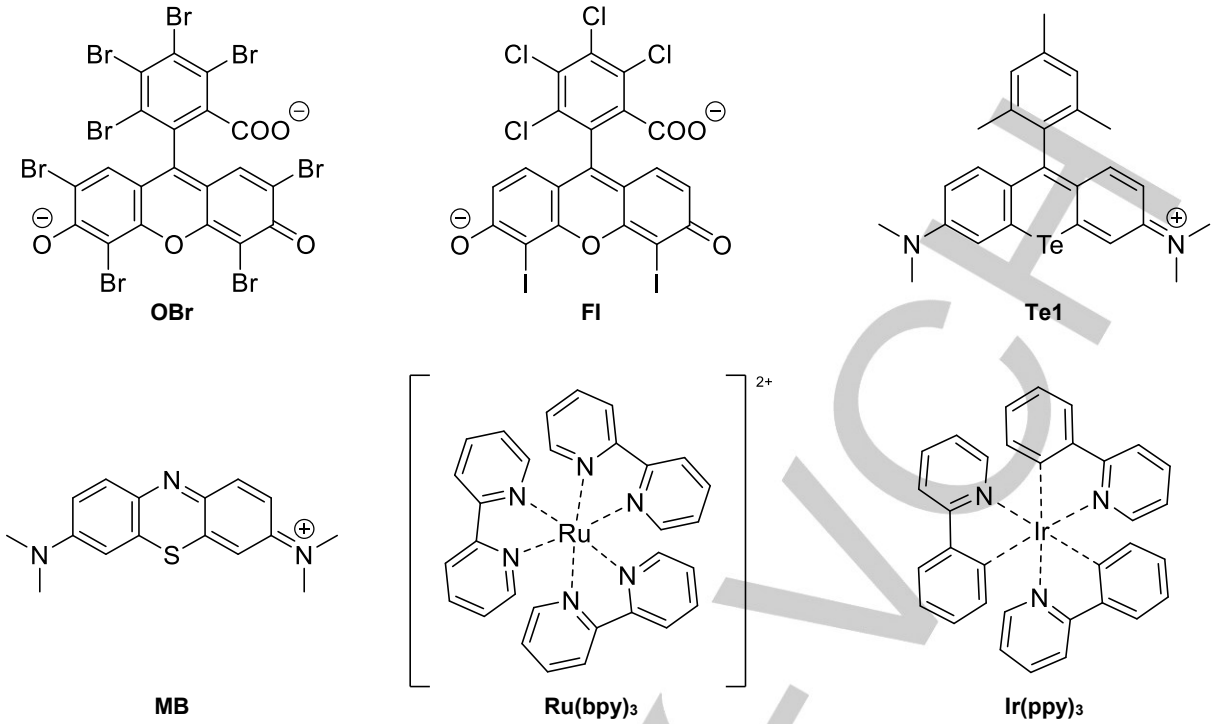

Figure 2. Compounds used to the test the model.

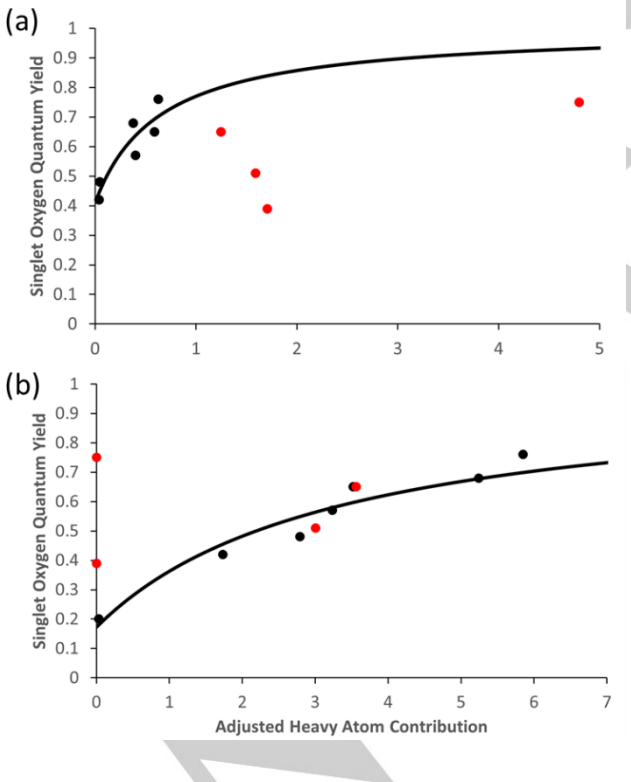

Figure 3. Experimental Φ_Δ against the calculated AHAC from the (a) LUMO and the (b) HOMO. A reciprocal trendline with an asymptote at 1 is shown, fit to the seven halogenated fluorescein derivates from Table 1 (black). These models did not work well with the test compounds, shown in red.

The structures of seven fluorescein derivatives were optimized using DFT. These derivatives were chosen because of their well characterized Φ_Δ and the variety and position of halogens in these structures. Using the optimized structures, the orbital populations were calculated using NBO. For these calculations we only consider atoms heavier than S and summed the atomic contribution of the heavy atoms in each orbital of interest. We then tested the model against other known chromophores shown in Figure 2.

Based on previous reports we initially only considered the AHAC to the LUMO.[9] A plot of the calculated AHAC to the LUMO against the experimental Φ_Δ revealed no trend (Figure 3a). Six of the fluorescein derivates (4,5-dibromo fluorescein, 4,5-diiodo fluorescein, 4,5-diiodo fluorescein, Eosin Y, Phloxine B, Erythrosine, and Rose Bengal) had calculated AHACs less than 1, whereas the 3',4',5',6'-tetrabromo fluorescein (**TBr**) had a value of 20.8 resulting in no acceptable way to fit a line to the data. After excluding the tetra-brominated derivative, a trend, including an asymptote at Φ_Δ=1, with a standard error equal to 0.048, was obtained. However, this model did not work well for other test compounds, as shown with the red dots in Figure 3a. Specifically, the two test halogenated fluorescein dyes, **OBr** and **FI**, had predicted Φ_Δ of 0.91 and 0.90, respectively. Compared to the experimental values of 0.65 and 0.55, there is a large difference between the predicted and experimental. Additionally, another test compound, **Te1**, has an experimental Φ_Δ of 0.75 which is extremely close to the Φ_Δ of Rose Bengal, 0.76.[15,16] Thus, we would expect these two compounds to have similar AHACs, yet the calculated AHAC is 0.62 for Rose Bengal and 4.80 for **Te1** using the LUMO. From this we concluded that the AHAC to the LUMOs cannot quantitatively predict the Φ_Δ of fluorescein derivatives, nor are they predictive for the Φ_Δ of other compounds

using this model, thus we turned to the AHACs of other frontier molecular orbitals.

The AHACs from the HOMOs of the chosen fluorescein dyes were plotted against the experimentally determined Φ_Δ (Figure 3b). This data could be fit with a trendline with a standard error of 0.043. The Φ_Δ of fluorescein derivatives are more dependent on the heavy atom contribution to their HOMOs. The test fluorescein derivates, **OBr** and **FI**, calculate a predicted Φ_Δ of 0.80 and 0.69, (experimental Φ_Δ of 0.65 and 0.55) respectively. While this is more accurate than the model based on the LUMO, it is not a strong enough correlation between the AHAC and Φ_Δ to use this as a predictive model. Furthermore, this model using the AHAC to the HOMO also fails at predicting the Φ_Δ of our other test compounds. For example, **Te1** has a predicted value 0.17, which is far less than the experimental Φ_Δ of 0.75.[16] The model also predicts a Φ_Δ of 0.17 for **MB**, where the experimental value is 0.39.[15] **Te1** and **MB** both have the same predicted Φ_Δ because both compounds have an AHAC from the HOMO that is approximately 0 and this model has a y-intercept at 0.17. Furthermore, it was counterintuitive that the HOMO would provide a better estimate of the Φ_Δ than the LUMO since the LUMO should be more involved in the excited state.

Both the HOMO and LUMO orbitals were calculated from the singlet ground state structure. We considered that the orbitals generated from a triplet calculation may yield better results. We modelled the lowest energy triplet state by optimizing the chemical structures in the triplet state. Using these structures, the AHAC was again determined using the NBOs. When a triplet state is calculated all orbitals are singly occupied. In the unrestricted triplet calculations, the Kohn-Sham orbital set is split into singly occupied alpha and beta orbitals. We started by looking at the lowest energy singly unoccupied molecular orbital (SUMO). In this case, the SUMO is a beta orbital. If one compares the singly occupied states of the triplet to the doubly occupied states of the singlet, the β-SUMO is comparable to the HOMO of the singlet state. The model created from the β-SUMO follows the pattern of the HOMO but with smaller values for the AHAC and a slightly higher standard error of 0.045, SI Figure S1. In an echo of the HOMO model, the β-SUMO version also fails to predict the Φ_Δ of non-fluorescein derivatives with the predicted Φ_Δ of **Te1** and **MB** falling short by 0.56 and 0.20, respectively. As with the HOMO, both dyes again have AHAC of approximately 0, thus their predictive Φ_Δ, 0.19, is the lowest value the model can predict. While the β-SUMO gives a decent trend, it is unclear as to why one would choose this orbital to model the Φ_Δ.

Thus, we investigated the triplet states associated with the LUMO. We broke this up into two potential models: the highest singly occupied molecular orbital (SOMO) and the SUMO+1. The SOMO is an alpha state while the SUMO+1 is the unoccupied beta state of the same orbital. Plotting the data generated from the SOMO does not create an observable correlation. A closer look at the values of the SOMO AHACs reveals that these orbitals have no ability to predict Φ_Δ. In this triplet orbital, Rose Bengal, Φ_Δ=0.76, and **Te1**, Φ_Δ=0.75, have largely different AHAC of 0.684 and 6.35, respectively.[15,16] For any of these models to have a predictive ability, the AHAC of these two dyes should be similar. The β-SUMO+1 is reminiscent of the LUMO; there is no observable correlation with the **TBr** included. **TBr** gives a β-SUMO+1 AHAC of 22.1 compared to the other fluorescein derivates that have AHACs with a maximum value of 0.777 for Rose Bengal. Excluding **TBr**, a decent trendline is obtained with a standard error equal to 0.048. However, this model fails to predict the Φ_Δ of other dyes due to the low AHAC in the fluorescein derivates compared to many other dyes. **Te1** and **MB** have β-SUMO+1 AHACs of 3.20 and 1.53 respectively, which are significantly greater than those of the fluorescein derivates in this model. The heavy atom contribution to the LUMO in both singlet and triplet states does not appear to be useful in predicting Φ_Δ.

A review of the triplet models reveals that the triplet orbitals did not add any new trends not already observed in the frontier orbitals from the singlet-state calculations. Additionally, the trend previously reported for TBT derivatives with the LUMO is not observed for fluorescein derivatives.[9] In the LUMO, the AHAC from most fluorescein dyes was an order of magnitude smaller than the contribution of non-fluorescein dyes with the exception of **TBr**, which had an AHAC of 20.8. The majority of the halogenated fluorescein derivates, **Ru(bpy)$_3$**, and **Ir(ppy)$_3$** had larger AHAC from the HOMO than that of the LUMO, contrary to the TBT derivatives, **Te1**, and **MB**. The correlation between the heavy atom contribution to the LUMO and Φ_Δ does not hold for all compounds nor does this correlation hold for the HOMO. However, all compounds have shown significant AHAC (<1) for either the HOMO or the LUMO. Considering this, we decided to take the sum of the AHAC for both frontier orbitals. A model created based on the sum of the AHAC of the HOMO and LUMO of the fluorescein derivates has one outlying data point, **TBr**. This derivate has the highest AHAC to the HOMO and LUMO, 20.8, combined with the lowest Φ_Δ of 0.20.

In the interest of understanding why the tetra-brominated fluorescein (**TBr**) behaved significantly different than the other fluorescein dyes, we started by investigating the frontier orbitals, visualized in SI Table S1. For most of the fluorescein derivates the HOMO is a π orbital and the LUMO is a π* on the xanthene ring. For **TBr**, on the other hand, the LUMO has all the orbital density on the brominated phenyl ring, visualized alongside Rose Bengal in Figure 4. Using TD-DFT calculations, the orbital contribution to the excitations was explored. For most fluorescein

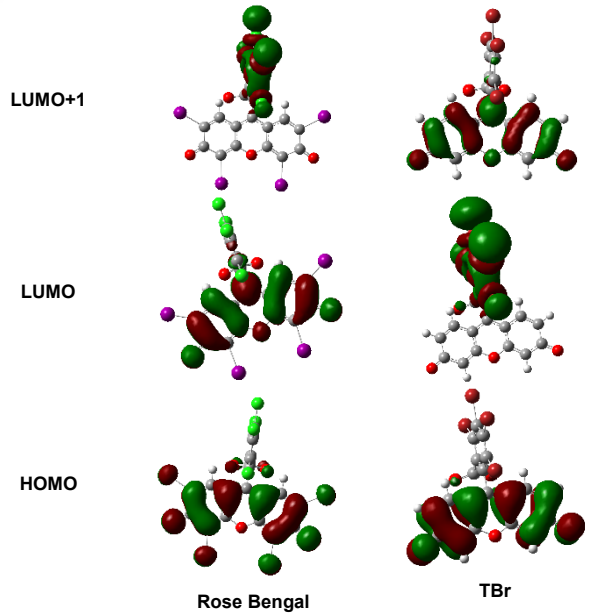

Figure 4. Computational derived orbital diagrams of the HOMO, LUMO, and LUMO+1 of Rose Bengal and **TBr**. The orbitals involved in the major transition for Rose Bengal are the HOMO and LUMO while the TBr is the HOMO and LUMO+1.

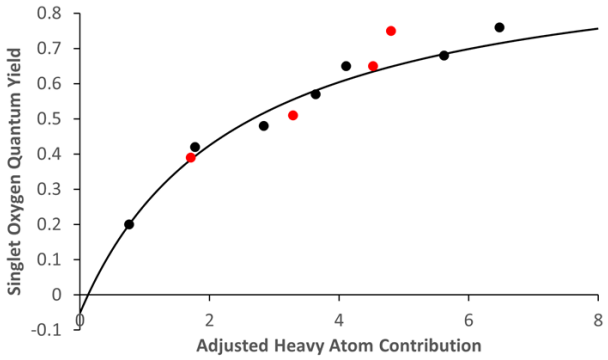

Figure 5. Experimental Φ_Δ against the calculated AHAC from the major contributing orbitals to the first excitation. A reciprocal trendline is fit to data from the seven halogenated fluorescein derivates from Table 1, shown in black (Equation 2). A good correlation with the test compound is shown in the red points.

derivatives the lowest energy allowed transition involves the HOMO → LUMO, $\pi \rightarrow \pi^*$ transition. For the **TBr** derivative the first major allowed transition is the HOMO to LUMO+1 rather than the HOMO to LUMO transition of the other derivates. The HOMO to LUMO+1 transition for **TBr** is the $\pi \rightarrow \pi^*$ transition, like the other dyes' lowest energy allowed transition. The localization of the orbital density on the LUMO and LUMO+1 for **TBr** are the reverse of Rose Bengal, with the **TBr** LUMO and Rose Bengal LUMO+1 showing orbital contribution from the halogenated phenyl ring. The AHAC using the sum of the HOMO and LUMO+1 for the **TBr** yields a much lower AHAC value from equation 1 of 0.76. Based on this, TD-DFT calculations were performed on the optimized structures for all of the dyes. From the TD-DFT calculations the orbitals with the largest co-efficient involved in the lowest energy transition with an oscillator strength over 0.1 were identified. A model made using a sum of the AHAC from the orbital pair involved in the transition produced a trendline Figure 5. This empirical formula, Equation 2, created from the experimental Φ_Δ and the computationally modelled AHAC of seven halogenated fluorescein derivates, is used to predict Φ_Δ.

$$\Phi_\Delta = 1 - \left(\frac{1}{0.393 \times (\mathrm{AHAC} + 2.417)}\right). \quad (2)$$

Where AHAC is the sum of the AHAC of the major orbitals involved in the first transition of a chromophore with an oscillator strength over 0.1 Major orbitals are chosen as the set of orbitals with the largest co-efficient for that transition. All values in this model are unitless, as quantum yield does not have units and the AHAC is a ratio adjusted by the associated atomic number(s). The model has a good correlation, σ_{est} of 0.028, with the fluorescein derivatives used in its creation and a is a non-linear function due to the asymptote fixed at Φ_Δ of 1. The model gave acceptable results, predicting Φ_Δ within 0.1 of the experimental Φ_Δ, for all compounds used to assess its predictive capabilities as shown in Table 2. This not only provides a model that fits this data set, but it also is not surprising that both of the orbitals involved in the first excited state should be the orbitals contributing to the Φ_Δ.

The function was forced to have an asymptote to reflect that a singlet-oxygen yield cannot be higher than 100%. However, this equation does not go to zero as the AHAC goes to zero as we would expect, instead reaching negative values of Φ_Δ at low AHAC. These negative values have no physical meaning as this model is created based on an approximation of the heavy atom effect and neglects contributions for atoms lighter than S; thus, a chromophore without any heavy atoms is outside the scope of this model.

Table 2. Lists the compounds used to the test model, including the AHAC, the predicted and experimental Φ_Δ, and associated error.

Compound	Adjusted Heavy Atom Contribution	Calculated Φ_Δ	Experimental Φ_Δ[15,16]	Φ_Δ Difference
OBr	4.52	0.63	0.65[a]	0.02
FI	3.29	0.55	0.51[a]	0.04
Te1	4.80	0.68	0.75[b]	0.07
MB	1.71	0.38	0.39[a], 0.51[b]	0.01, 0.13
Ru(bpy)$_3$	36.7	0.93	0.90[b]	0.03
Ir(ppy)$_3$	38.4	0.94	1[b]	0.06

[a] Measured in H_2O. [b] Measured in MeOH

Testing the predictive capabilities

We initially tested the predictive power of the model with extremely similar chromophores. Two novel fluorescein derivatives, **OBr** and **FI**, were synthesized for this purpose. Using this model, the predicted Φ_Δ of **OBr** and **FI** were 0.63 and 0.55, respectively. These are within experimental error of the experimentally determined Φ_Δ of 0.65 and 0.51, respectively, confirming that this model is predictive for Φ_Δ for very similar chromophores. The **OBr** dye had similar orbital order to the **TBr**; the first transition occurs between the HOMO and LUMO+1, as visualized in SI Table S2. The use of the orbitals contributing to the first excitation supports our theory that it is not just the AHAC to the HOMO or LUMO that determine Φ_Δ.

To explore the use of our model on chromophores with more exotic structures we examined a mesityl tellurorhodamine dye (**Te1**) and methylene blue (**MB**). **Te1** was originally chosen as it is a dye frequently used within our lab and because rhodamine dyes are relatively similar to fluorescein dyes. Both the **Te1** and **MB** differ from the fluorescein derivatives in that they only contain one heavy atom, which is contained in the ring structure. Also, both the **Te1** and **MB** have a positive charge instead of the negative two charge of fluorescein. **MB** further differs from the fluorescein dyes with the removal of the upper phenyl ring. As an additional stressor, the heaviest atom in **MB** is sulfur, an atom not generally considered to be heavy. The model does well with both dyes, as seen in Table 2, the predicted Φ_Δ of **Te1** and **MB** are 0.68 and 0.38, respectively, similar to the experimental values of 0.75 in MeOH and 0.39 in water, respectively, further supporting the predictive power of the model.[15,16] The experimental Φ_Δ in the case of the **Te1** dye was determined in MeOH whereas all the fluorescein derivates were determined in water and all computations were completed in vacuum. The role of solvent is discussed in more depth below.

Many triplet chromophores are octahedral transition metal complexes with structures and photophysics significantly different from the chromophores used to build the model. Among the most extensively studied is **Ru(bpy)$_3$**. Surprisingly the model predicts the Φ_Δ of 0.93 for **Ru(bpy)$_3$**, within 0.03 of the experimental value

of 0.90 measured in MeOH.[15] This ruthenium complex has a weak oscillator strength of the first transition, 0.103, often associated with degeneracy. There are three sets of orbitals involved in the excitation, two with roughly 35% probability and the third at 24%. The DFT calculated alpha eigenvalues show two important sets of degeneracy: the HOMO-2, HOMO-1 and LUMO+1, LUMO+2 with energies of -11.39 and -7.69 eV, respectively, visualized in Figure 6. The HOMO and LUMO are slightly closer in energy at -11.22 and -7.79 eV, respectively. This orbital splitting pattern matches what we would expect for the bidentate ligand system as the bite angle causes **Ru(bpy)$_3$** to have a D_3 symmetry point group.[17] The two highest probability excitations for **Ru(bpy)$_3$** are the degenerate dπ to dπ* excitations between the HOMO-2 to LUMO+1 or HOMO-1 to LUMO+2, at 35.1% and 35.0%, respectively. Due to the degeneracy causing a lack of a preferred excitation, we planned to use the normalized, weighted average of the AHAC for both degenerate contributing orbitals of **Ru(bpy)$_3$**. However, both transitions give equal predicted Φ_Δ of 0.93 meaning that the normalized, weighted average has no change to the predicted value of this compound compared to just choosing one set of the degenerate orbitals.

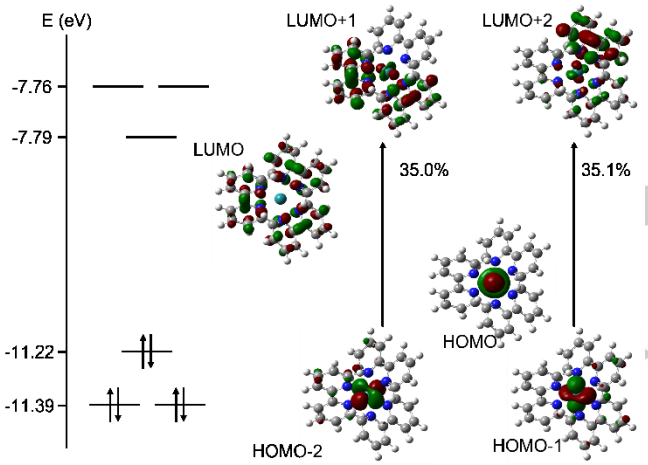

Figure 6. An orbital density diagram showing the degeneracy observed in **Ru(bpy)$_3$** including the probability, in percent, for the excitation to occur between these orbitals. This excitation state for **Ru(bpy)$_3$** has an oscillator strength of 0.1030 and excitation energy of 422.39 nm.

To further investigate how this model applies to transition metal complexes, we also investigated **Ir(ppy)$_3$**. Through the model, **Ir(ppy)$_3$** has a predicted Φ_Δ of 0.94; a 0.06 difference from the experimental Φ_Δ of approximately 1 in MeOH.[15] **Ir(ppy)$_3$** is similar to **Ru(bpy)$_3$** from a ligand field theory viewpoint, as the Ir is a d_6 metal with three bidentate ligands. As with the **Ru(bpy)$_3$** complex, we expected and observed two sets of degeneracy for **Ir(ppy)$_3$** in the HOMO-2 and HOMO-1 and LUMO+1 and LUMO+2. For **Ir(ppy)$_3$**, the HOMO-2 and HOMO-1 have energies equal to -1.54 eV, the HOMO at -1.64 eV, the LUMO at -5.16 eV, and the LUMO+1 and LUMO+2 at -5.32 eV as visualized in SI Figure S2. The two degenerate most probable excitations are the HOMO-2 to LUMO+1 and HOMO-1 to LUMO+2 with probabilities equal to 43.3% and 40.9%. Like **Ru(bpy)$_3$**, both degenerate excitations yield the same AHAC and Φ_Δ. The degeneracies of the orbitals involved in the first transition of these metal complexes makes it more difficult to select the major transition. However, degenerate orbital sets yield equal values for the AHAC and can be identified without any further computations or calculations required.

Solvent Effects

This model does not consider solvent effects. Experimental Φ_Δ can vary wildly depending on the solvent.[6b] Additionally, the method used to determine Φ_Δ can also lead to inconsistencies within reported experimental values. For example, **Ru(bpy)$_3$** has experimentally reported Φ_Δ of 0.22 in H_2O, 0.83-0.9 in MeOH, and 0.73 in EtOH.[6b,15] **MB** has reported Φ_Δ ranging from 0.35 to 0.70 depending on method, solvent, *etc*.[15] This predictive model was created based on fluorescein derivatives where the calculations were completed in vacuum, while the experimental Φ_Δ were measured in basic water. We found that the model is accurate for predicting the Φ_Δ of **MB**, which is experimentally reported in water, while **Te1**, **Ru(bpy)$_3$**, and **Ir(ppy)$_3$** all match experimental values obtained in MeOH. Since **Ru(bpy)$_3$** has large solvent effects in its Φ_Δ, it was chosen to test the role of solvents in the calculations. We used two implicit solvation models: water and methanol and optimized the structure of **Ru(bpy)$_3$** and determined the AHAC. The calculated AHAC for **Ru(bpy)$_3$** in vacuum, water, and methanol were 36.0, 35.9, and 35.9, respectively. The difference between the AHACs is too small to make a significant change to the predicted Φ_Δ with all three models predicting Φ_Δ of 0.93 when the AHAC was put into the model. Thus, it was determined that the values calculated in vacuum were sufficient, and that any solvent effects causing the observed differences are not captured with the implicit solvent model. To keep the model as simple as possible, no solvation models were applied to the remaining calculations. Additionally, adding solvent systems increases the computational cost and knowledge required to utilize the model, which is counter to our proposed purpose.

Uses for the model

This model was derived by investigating an approximation of the heavy atom effect with the goal that it would be able to aid in directing the future synthesis of new chromophores. While it can accurately predict the Φ_Δ of chromophores, it is most useful in identifying how changes will affect a set of chromophores. The model can help identify the effect of heavy atom containing functional groups on given positions on a chromophore. Investigating the fluorescein derivates through the model, we can determine that halogens on the upper phenyl ring have a smaller impact on the Φ_Δ than halogens attached to the conjugated xanthene ring structure. The ability to use the model to locate functional group position that will have the largest effect on the Φ_Δ is extremely useful when designing a targeted dye. Alternatively, it can be used to probe the effects differing functional groups will have on the same location of dye. Overall, we hope this can minimize synthetic effort through computational design. Using this model involves three computations and two equations. One needs to optimize the compound, then complete a TD-DFT and NBO energy calculations. The heavy atom contribution to the major orbitals (identified from the TD-DFT calculation) is obtained from the NBO calculation, we used the Multiwfn program.[12] The AHAC is calculated through Equation 1, and then entered into Equation 2 to yield the calculated Φ_Δ (more detail for these steps are provided in the Supporting Information).

Conclusion

We have created a predictive model for Φ_Δ based on an approximation of the heavy atom effect and the experimental Φ_Δ of several halogenated fluorescein derivatives. The creation of this model supports that both the position and identity of heavy atoms are important factors when determining the Φ_Δ of heavy atom containing chromophores. Additionally, the frontier orbitals are not always the most important orbitals when optimizing the Φ_Δ as the HOMO to LUMO transition is not always involved in the first excitation. This model can help identify how structural changes will influence efforts in tuning a chromophore to enhance or diminish the triplet yield. By using the adjusted heavy atom contribution (AHAC), we avoid computationally expensive ISC and SOC calculations. However, this means that this model is created based solely on an approximation of the heavy atom effect; a reliance that limits the scope of the model to heavy atom (arbitrarily chosen as any atom larger than S) containing chromophores. This simplification makes the model extremely useful in its intended purpose as a screening tool for designing new photosensitizers as it can quickly predict the Φ_Δ of new chromophores. This model has been shown to accurately calculate the Φ_Δ of fluorescein derivatives, rhodamine derivatives, and octahedral metal complexes. This model is a useful tool for the preliminary design of new chromophores as well as for gaining a better understanding of the impact of changing functional groups on a chromophore.

Experimental Section

Tetrachlorophthalic anhydride and potassium iodide were commercially purchased through Sigma-Aldrich, Sodium Bicarbonate from VWR Analytic, and DMSO-d_6 was obtained from Acros Organics. Reagent grade chemicals of rescorinol, zinc chloride, sodium sulfate, dichloromethane, diethyl ether, and N-iodosuccinimide were used.

Synthesis of 3',4',5',6'-tetrachloro fluorescein

3',4',5',6'-tetrachloro fluorescein was synthesized by a solid-state reaction previously reported.[18] Tetrachlorophthalic anhydride (5.091 g, 17.86 mmol) was ground with 2 eq. of resorcinol (3.862 g, 35.10 mmol) and $ZnCl_2$ (0.680 g, 5.01 mmol) as a catalyst. The mixture was then heated in a sand bath (140 °C) under nitrogen flow for 40 minutes. While still warm, MeOH (90 mL) was added and sonicated until all solid was dissolved. Water (270 mL) was then added, and the precipitated product was obtained via vacuum filtration. The filtered product (7.455 g, 88 % yield) was then dried by oven (60 °C) overnight. ^{1}H NMR (400 MHz, DMSO-d_6): δ 10.27 (s, 1H), 7.00 (d, J = 8.7 Hz, 1H), 6.74 (d, J = 2.4 Hz, 1H), 6.62 (dd, J = 8.7, 2.4 Hz, 1H).

Synthesis of Fl

To tetrachloro fluorescein (0.133 g, 0.283 mmol), saturated $NaHCO_3$ (6.3 mL) and KI (4 mL, 0.1 M) solution were added. N-iodosuccinimide (0.124 g, 0.552 mmol) was added and refluxed for 30 minutes under nitrogen flow, then cooled to room temperature. 4 M HCl was added dropwise until a secession of effervescence was observed. Product was obtained via DCM extraction (3x25 mL). The combined organic extracts were washed with brine, dried with Na_2SO_3, and condensed. Product was purified via a silica column and a DCM/diethyl ether gradient provided Fl (0.064 g, 24% yield). ^{1}H NMR (400 MHz, DMSO-d_6): δ 11.10 (s, 1H), 7.01 (d, J = 8.7 Hz, 1H), 6.72 ppm (d, J = 8.7 Hz, 1H). ^{13}C NMR (400 MHz, DMSO-d_6) δ 179.91, 163.61, 160.54, 152.62, 147.83, 139.50, 135.63, 130.97, 128.98), 127.77, 124.83, 112.22, 108.24, 74.83 ppm. HRMS (ESI): m/z calcd for $C_{20}H_5Cl_4I_2O_5^-$: 720.6945; found: 720.6959.

Synthesis of OBr

Tetrabromo fluorescein (0.652 g, 1.01 mmol) was dissolved in ethanol (5 mL) in a cool water bath. To this solution 9 eq. of Br_2 was added and stirred for 30 minutes. The solution was allowed to sit overnight, and the precipitate was isolated by vacuum filtration then dried in an oven overnight. The resulting product was pink powder. (0.685 g, 73% yield). ^{1}H NMR (400 MHz, DMSO-d_6): 10.83 (s, 1H) and 7.51 ppm (s, 1H). ^{13}C NMR (400 MHz, DMSO-d_6): 80.50, 100.65, 102.47, 107.92, 110.68, 127.72, 130.26, 133.61, 137.26, 148.49, 149.77, 154.07, 163.97, and 166.02 ppm. HRMS (ESI): m/z calcd for $C_{20}H_3Br_8O_5^-$: 962.3360; found: 962.3361.

General methods for determination of photophysical properties

UV-Vis spectra were recorded using a Shimadzu StellarNet SILVER-Nova25 BW16 spectrometer and quartz cuvettes. Stock solutions of OBr and Fl (10^{-5} M) were created in phosphate buffer saline (pH 7.4). The Φ_Δ were determined by the rate of oxygen consumption in DMSO as previously described using Rose Bengal as a standard (Φ_Δ= 0.76).[14]

Computation Details

All calculations were completed with Gaussian09 input files and visualized through GaussView05.[19] All structures were optimized in singlet and triplet states at a B3LYP level of theory with the 6-311+G(d) basis set for bromide and smaller atoms, and LANL2DZ for I, Ru, Ir, and Te. The excitation was chosen as the lowest energy excitation with an oscillator strength greater than 0.1, calculated through TD-DFT for 20 states. The orbital pair with the highest co-efficient contributing to this excitation was selected as the major orbitals for determining the AHAC. Degeneracy was determined through SCF density population analysis. A NBO energy calculation was completed to determine the atomic orbital contribution to each molecular orbital using the keywords density=current and pop=nboread. From here the heavy atom contributions–for any atom greater than sulfur–were determined by the Multiwfn program using the natural atomic orbital contribution set to show all natural atomic orbitals and/or shells.[12]

The supporting information contains more detailed methods for using the model as well as figures of the unsuccessful models (β-SUMO) and extended computational data on the fluorescein derivatives and test compounds (energy, oscillator strength, transition probability, orbital density diagrams).

Acknowledgements

This work was funded by the American National Science Foundation, Directorate for Mathematical and Physical Science, Division of Chemistry, award #1800599. The National Science Foundation is acknowledged for support of the BioAnalytical Mass Spectrometry Facility at PSU (MRI 1828573). Funding was also provided from the Portland State University Faculty Development Grant.

Keywords: triplet-quantum-yield • Heavy atom effect • singlet oxygen • phosphorescence • intersystem crossing

[1] a) E. Rivard, *Chem. Lett*. **2015**, 44, 730–736; b) K. M. Farrell, M. M. Brister, M. Pittelkow, T. I. Sølling, C. E. Crespo-Hernández, *J. Am. Chem. Soc*. **2018**, 140, 11214–11218; c) B. Minaev, G. Baryshnikov, H. Agren, *Phys. Chem. Chem. Phys*. **2014**, 16, 1719–1758, d) A. I. Rodrigues, P. Krishnamoorthy, C. S. B. Gomes, N. Carmona, R. E. Di Paolo, P. Pander, J. Pina, J. Sérgio Seixas de Melo, F. B. Dias, M. J. Calhorda, A. L. Maçanita, J. Morgado, P. T. Gomes, *Dalton Trans*. **2020**, 49, 10185–10202.

[2] a) J. Zhang, S. Mukamel, J. Jiang, *J. Phys. Chem. B* **2020**, 124, 2238–2244; b) J. Zhao, W. Wu, J. Sun, S. Guo, *Chem. Soc. Rev*. **2013**, 42, 5323–5351.

[3] R. P. Sabatini, T. M. McCormick, T. Lazarides, K. C. Wilson, R. Eisenberg, D. W. McCamant, *J. Phys. Chem. Lett.* **2011**, 2, 223–227.

[4] G. R. Fleming, A. W. E. Knight, J. M. Morris, R. J. S. Morrison, G. W. Robinson, *J. Am. Chem. Soc.* **1977**, 99, 4306–4311.

[5] a) S. P. McGlynn, R. Sunseri, N. Christodouleas, *J. Chem. Phys.* **1962**, 37, 1818-1824; b) J. C. Koziar, D. O. Cowan, *Acc. Chem. Res.* **1978**, 11, 334–341.

[6] a) J. N. Demas, E. W. Harris, R. P. McBride, *J. Am. Chem. Soc.* **1977**, 99, 3547–3551; b) M. I. Gutiérrez, C. G. Martínez, D. García-Fresnadillo, A. M. Castro, G. Orellana, A. M. Braun, E. Oliveros, *J Phys. Chem. A* **2003**, 107, 3397–3403.

[7] a) M. R. Detty, P. B. Merkel, *J. Am. Chem. Soc.* **1990**, 112, 3845–3855; b) E. Pomarico, P. Pospíšil, M. E. F. Bouduban, J. Vestfrid, Z. Gross, S. Záliš, M. Chergui, A. Vlček, *J. Phys. Chem. A* **2018**, 122, 7256–7266.

[8] H. Shi, L. Song, H. Ma, C. Sun, K. Huang, A. Lv, W. Ye, H. Wang, S. Cai, W. Yao, Y. Zhang, R. Zheng, Z. An, W. Huang, *J. Phys. Chem. Lett.* **2019**, 10, 595–600.

[9] R. Acharya, S. Cekli, C. J. Zeman, R. M. Altamimi, K. S. Schanze, *J. Phys. Chem. Lett*. **2016**, 7, 693–697.

[10] a) T. L. D. Tam, T. T. Lin, H. M. Chua, *Phys. Chem. Chem. Phys*. **2017**, 19, 15671–15675; b) B. de Souza, G. Farias, F. Neese, R. Izsák, *J. Chem. Theory Comput.* **2019**, 15, 1896–1904; c) E. Y. Li, T. Jiang, Y. Chi, P. Chou, *Phys. Chem. Chem. Phys*. **2014**, 16, 26184–26192; d) I. Kim, W.-J. Son, Y.-S. Choi, A. Osipov, D. Lee, H. Lee, Y. Jung, J. Son, H. Choi, W. Sotoyama, A. Yakubovich, J. Shin, H. S. Lee, *J. Phys. Chem. C* **2019**, 123, 11140–11150.

[11] a) M. W. Kryman, G. A. Schamerhorn, J. E. Hill, B. D. Calitree, K. S. Davies, M. K. Linder, T. Y. Ohulchanskyy, M. R. Detty, *Organometallics* **2014**, 33, 2628–2640; b) R. Liu, X. Gao, M. Barbatti, J. Jiang, G. Zhang, *J. Phys. Chem. Lett.* **2019**, 10, 1388–1393; c) Y. P. Rey, D. G. Abradelo, N, Santschi, C. A. Strassert, R. Gilmour, *Eur. J. Org. Chem.* **2017**, 2017, 2170–2178.

[12] T. Lu, F. Chen, *J. Comput. Chem.* **2012**, 33, 580–592.

[13] C. M. Marian, *WIREs Comput Mol Sci* **2012**, 2, 187–203.

[14] L. V. Lutkus, S. S. Rickenbach, T. M. McCormick, *J. Photochem. Photobiol. A Chem.* **2019**, 378, 131–135.

[15] F. Wilkinson, W. P. Helman, A. B. Ross, *J. Phys. Chem. Ref. Data* **1993**, 22, 113–262.

[16] M. W. Kryman, G. A. Schamerhorn, K. Yung, B. Sathyamoorthy, D. K. Sukumaran, T. Y. Ohulchanskyy, J. B. Benedict, M. R. Detty, *Organometallics* **2013**, 32, 4321–4333.

[17] C. I. Oprea, B. Frecuş, B. F. Minaev, M. A. Gîrţu, *Mol. Phys.* **2011**, 109, 2511–2523.

[18] N. Pietrancosta, A. Kessler, F.-C. Favre-Besse, N. Triballeau, T. Quentin, B. Giros, S. El Mestikawy, F. C. Acher, *Bioorganic Med. Chem*. **2010**, 18, 6922–6933.

[19] a) Gaussian 09, Revision D.01, M. J. Frisch, G. W. Trucks, H. B. Schlegel, G. E. S.; M. A. Robb, J. R. Cheeseman, G. Scalmani, V. Barone, B. M.; G. A. Petersson, H. Nakatsuji, M. Caricato, X. Li, H. P. H.; A. F. Izmaylov, J. Bloino, G. Zheng, J. L. Sonnenberg, M. H.; M. Ehara, K. Toyota, R. Fukuda, J. Hasegawa, M. Ishida, T. N.; Y. Honda, O. Kitao, H. Nakai, T. Vreven, J. A. Montgomery, J.; J. E. Peralta, F. Ogliaro, M. Bearpark, J. J. Heyd, E. B.; K. N. Kudin, V. N. Staroverov, T. Keith, R. Kobayashi, J. N.; K. Raghavachari, A. Rendell, J. C. Burant, S. S. Iyengar, J. T.; M. Cossi, N. Rega, J. M. Millam, M. Klene, J. E. Knox, J. B. C.; V. Bakken, C. Adamo, J. Jaramillo, R. Gomperts, R. E. S.; O. Yazyev, A. J. Austin, R. Cammi, C. Pomelli, J. W. O.; R. L. Martin, K. Morokuma, V. G. Zakrzewski, G. A. V.; P. Salvador, J. J. Dannenberg, S. Dapprich, A. D. D.; O. Farkas, J. B. Foresman, J. V. Ortiz, J. C.; Fox, D. J. Wallingford CT **2013**; b) GaussView, Version 5, Roy Dennington, Todd A. Keith, and John M. Millam, Semichem Inc., Shawnee Mission, KS, **2009**.

Entry for the Table of Contents

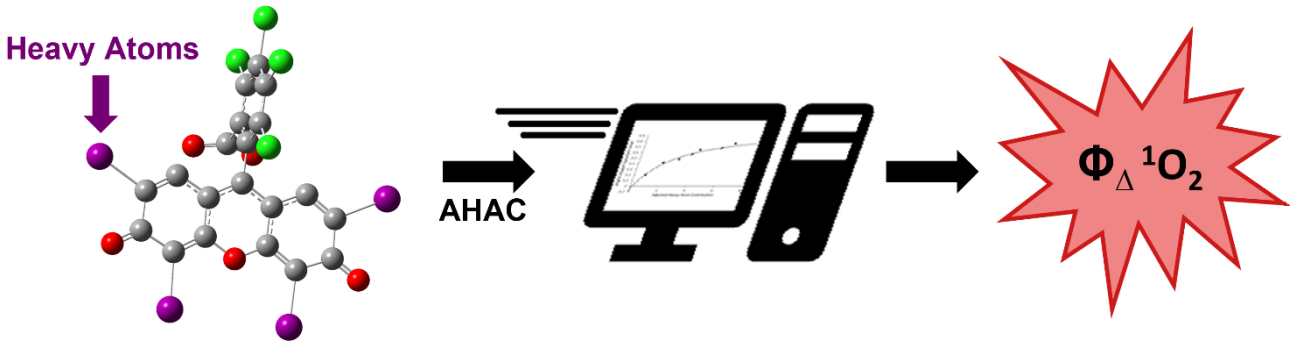

A simple DFT based model that can be used to predict triplet-yields has been tested against a variety of chromophores including rhodamine dyes, fluorescein derivatives, and octahedral metal complexes.